World Academy of Science, Engineering and Technology
International Journal of Mechanical and Mechatronics Engineering
Vol:8, No:11, 2014

Numerical Study on the Static Characteristics of Novel Aerostatic Thrust Bearings Possessing Elastomer Capillary Restrictor and Bearing Surface

S. W. Lo, S.-H. Lu, Y. H. Guo, L.-C. Hsu

***Abstract*—**In this paper a novel design of aerostatic thrust bearing is proposed and is analyzed numerically. The capillary restrictor and bearing disk are made of elastomer like silicone and PU. The viscoelasticity of elastomer helps the capillary expand for more air flux and at the same time, allows conicity of the bearing surface to form when the air pressure is enhanced. Therefore the bearing has the better ability of passive compensation. In the present example, as compared with the typical model, the new designs can nearly double the load capability and offer four times static stiffness.

***Keywords*—**Aerostatic, bearing, elastomer, static stiffness.

I. Introduction

IN spite of the relatively low stiffness and load capacity as compared to roller and hydrostatic bearings, aerostatic thrust bearings have been employed widely in coordinate measurement and ultra-precision machining due to their high accuracy and near-frictionless running characteristics [1]. To overcome the disadvantages, which mainly result from the compressibility of air medium, both passive and active approaches have been carried out.

Al-Bender [2] proved that there are various possibilities of applying active compensation to air bearings and result in considerable enhancing their static and dynamic performances. For example, it is well known that a converging (concave) bearing surface is able to level up the load capacity; therefore, in Al-Bender studies, piezoelectric actuators were arranged in different ways to control the film geometry such as the gap height and the conicity of the bearing surface. Profound gain per actuator displacement and very large bandwidth of the active air film can be obtained. Infinite static stiffness is also realized using integrative action in the controller. However, as pointed out by Aguirre etc. [3], though the laboratory results are promising, the step to industrial application has not been achieved yet, due to a combination of several reasons, e.g. the high added cost of active components including sensors, actuators, amplifiers, data processing units, etc.

On the other hand, by further optimizing the passive solutions, the design requirements of the bearing functions may be fulfilled without complex controlling units and expensive components. For instance: modifying the air flow [4], using porous material [5] or similar material like woven wire cloth [6] can improve the pressure distribution for better stiffness, reduce the vibration, or eliminate the resonance of bearing with the stimulating force.

In the present paper, we intend to propose a novel design composed of polymers. The viscoelastic nature of polymers adds particular benefits to the bearing design in several aspects. Firstly, the capillary restrictor is made of soft elastomer like silicone for sensitive response to the variation of cell pressure. It is well known that the impedance of the capillary is inversely proportional to the capillary radius to the fourth power. Therefore a tiny expansion of the capillary may lead to considerable passive compensation of the air flux. Secondly, the flexible polymer bearing surface is easily to form a converging profile automatically by the film pressure to increase the load capability. Moreover, Kwan and Post [1] showed that the manufacturing errors on aerostatic bearing surfaces and orifice geometry are known to impair performance. However, the elastic deformation of the polymer potentially alleviates the sensitivity of load and stiffness to various forms of manufacturing error. Thirdly, the viscous energy dissipation might provide additional damping to the bearing system. For instance, pocketed orifice bearings give higher load capacity as compared to inherently compensated orifice type bearing, also known as laminar flow restrictor; nevertheless it is prone to pneumatic hammering under cyclic, dynamic load. We expect that the viscoelastic polymer will bring in extra damping to stabilize the oscillation.

II. Description of Structure and Material

The thrust bearings system are shown by the axisymmetric cross sections as shown in Fig. 1 where bulk 1 is the counter surface, region 2 denotes the air pocket (cavity), components 3 and 4 belong to the bearing body, and region 5 indicates the hollow chamber surrounding the polymer tube. All the 60 mm-diameter thrust bearings have an inlet hole of 2 mm diameter and a 1.8 mm-long capillary of 0.2 mm diameter, following a pocket of 2 mm diameter and 1 mm deep. Three different types of the inner structures are named: “straight”, “confined”, and “free” tubes according to the shape of or the

S. W. Lo is with the Department of Mechanical Engineering, National Yunlin University of Science and Technology, Douliou City, 640 Yunlin, Taiwan (phone: +886-5-5342601 ext. 4140; fax: +886-5-5312062; e-mail: losw@ yuntech.edu.tw).

S. H. Lu and Y. H. Guo are with the Department of Mechanical Engineering, National Yunlin University of Science and Technology, Douliou City, 640 Yunlin, Taiwan (e-mail: m10111056@yuntech.edu.tw, m10111009@ yuntech.edu.tw, respectively.).

L. C. Hsu is with the Department of Mechanical Engineering, National Yunlin University of Science and Technology, Douliou City, 640 Yunlin, Taiwan (phone: +886-5-5342601 ext. 4151; fax: +886-5-5312062; e-mail: edhsu@ yuntech.edu.tw).

restriction on component 3 containing the air channel. The straight type is the easiest one to make. The confined type can joint component 3 with body 4 which has different material property, usually harder, near the air pocket. The free type allows the capillary to expand easier; however, it needs more steps to mold. In the present study, the inner and outer diameters of the hollow chamber (region 5) are set as 4 mm and 5 mm, respectively.

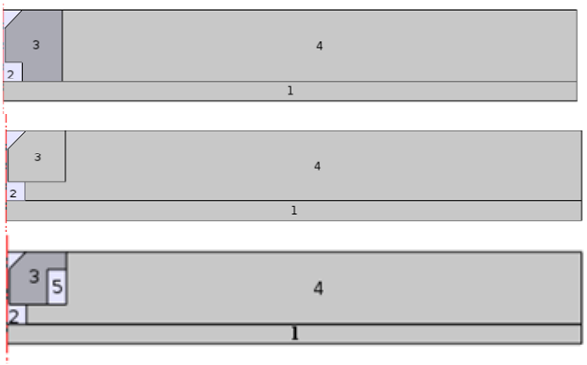

Fig. 1 Cross sections of bearing and counter surface. Top to bottom are types of straight, confined, and free tube, respectively

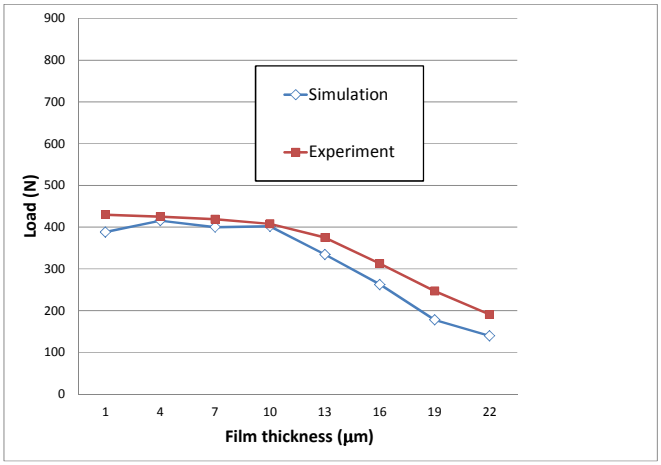

Fig. 2 Comparison between numerical and experimental [7] results

TABLE I
MATERIAL PROPERTIES AND NOTATIONS FOR SIMULATION

TYPE	MATERIAL PROPERTY			
	3	4	5	Young's modulus:
Typical	AL6061	AL6061	-	SI= 3.44
Confined-tube/SI-SI	SI	SI	-	SI'= 34.4
Confined-tube/SI-SI'	SI	SI'	-	PU= 275
Confined-tube/SI-PU	SI	PU	-	(MPa)
Free-tube/SI-SI	SI	SI	Air	Poisson ratio:
Free-tube/SI-SI'	SI	SI'	Air	SI= 0.48
Free-tube/SI-PU	SI	PU	Air	SI'= 0.48
Straight-tube/SI-PU	SI	PU	-	PU= 0.18

The materials used for various regions are listed in Table I, including two kinds of silicones with different Young's modulus and one kind of PU. The softer silicone is denoted as SI while the harder one is marked by SI'. The structures without the hollow chamber, either the straight or the confined tube, can be used to simulate the so called "typical" bearing since components 3 and 4 are "united" as one piece made of AL6061.

III. Simulation Procedures

The commercial code COMSOL is used for the simulation. Firstly, the code offers the options of various mesh densities for simulation and therefore the most efficient one should be found before starting our numerical experiments. Table II shows the loads calculated for the typical bearing with film thickness (gap between bearing and counter surface) equal to 30 microns using different degrees of discretization, from extremely rough to extremely fine. It can be seen that the choice of element size does not affect the result significantly and the "normal" setting, which is generated automatically by the system is satisfactory. Too many elements will not only consume too much computing time but also, under certain circumstance, inducing extra computing errors due to the very tiny elements. Furthermore, to prove the validity of the simulation, the code is then adopted to calculate the load-film thickness relations for the experiment conducted by Li and Ding [7]. The comparison is given in Fig. 2 and the discrepancy is acceptable. In the following section, components 3 and 4 are fixed on their upper boundaries and are united while the counter surface is immobile on its lower edge. The air fills in the chamber with its pressure gradually enhanced to 0.5 MPa (5 bar) at the top of region 2 and flows through the gap between components 1 and 4 to the brink of the disk where the pressure drops to zero. For each given film thickness (thickness of the gap) the calculated pressure is integrated to get the load capacity of the bearing. The stiffness for each film thickness is approximated by typical finite difference skill.

IV. Results and Discussions

In all the cases, expect for the typical one, block 3 is made of the soft silicone for superior flexibility. Figs. 3 and 4 show the load capability and static stiffness for bearings of various structures and material combinations. All the bearings exhibit similar performance when the load is under about 120 N. Beyond this point, increasing air pressure forces the elastic capillary to expand to augment the air flux. It is obviously that the free tube works better than the other two types. Moreover, the capability of the S-type is close to that of the C-type.

TABLE II
SETTINGS OF MESH FOR SIMULATION (COMSOL DEFAULT SETTING)

Gap h = 30 μm	Extremely coarse mesh	Extra coarse mesh	Coarser mesh	Coarse mesh
Load (N)	35.788	30.937	32.15	31.995
Element number	13678	19169	22179	21314
Maximum element size	2.91 mm	1.72 mm	1.15 mm	0.886 mm
Minimum element size	0.926 mm	0.662 mm	0.529 mm	0.397 mm
Gap h = 30 μm	Normal mesh	Fine mesh	Finer mesh	Extremely fine mesh
Load (N)	33.384	33.267	30.135	28.855
Element number	29125	34240	43295	209189
Maximum element size	0.595 mm	0.463 mm	0.37 mm	0.0886 mm
Minimum element size	0.265 mm	0.132 mm	0.0529 mm	0.00265 mm

When the soft silicone SI is used for both block 3 and disk 4, the disk surface deforms so seriously that it becomes incapable of constraining the air flow to engender higher pressure. The load capacity and stiffness are therefore even inferior to that of the typical design. Simply replacing the softer silicone with a "harder" one, SI', for the disk can surprisingly improve the load capability from 400 N (typical design) to more than 700 N at film thickness 5 μm. The most remarkable progress in static stiffness, which climbs from 21 N/μm to 76 N/μm, is found to occur at film thickness 10 μm where the load capability also ascents form 300 N to 500 N. Fig. 5 shows the deformed polymer structure near the center of the free-tube/SI-SI' bearing for film thicknesses equal to 20 and 5 μm respectively. The expansion of the silicone tube is apparent. Their pressure profile along the radial direction, from the center to the rim of the disk, is shown in Fig. 6. The axial (longitudinal) displacement of the bearing surface (measured from the air pocket edge to the disk outer rim, total 29 mm) is given by Fig. 7. Obviously the bearing surface is pushed inside by the air to form a concave shape that retards the drop of air pressure. In the case of 5 micron gap, the pressure can even be kept nearly as high as the supplied 0.5 MPa within a circular area of radius 3 mm, which is much larger than the area of the air pocket. The hollow chamber (region 5) not only induces more expansion of the capillary but also help in curving the surface. The remaining part of disk 4 also provides a concaved surface to build up the pressure.

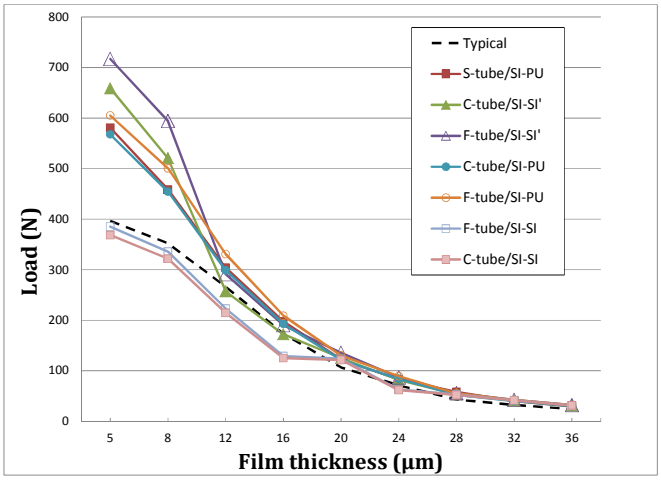

Fig. 3 Load capacity vs. film thickness for various bearing structures and materials (S= straight; C= confined; F= free)

Another interesting finding from Fig. 3 is that, when the Young's modulus of disk 4 increases further to that of the typical PU, its load capability transcends the SI-SI' type for film thickness between 12 μm and 20 μm, but the SI-SI' takes the lead when the gap goes down below 12 μm. It implies that depending on the designed working film thickness, there is an optimal choice regarding the materials for block and disk to attain the most plump pressure distribution. This will be our future work.

In conclusion, the free-tube configuration together with the SI-SI' combination of material can offer the better load ability as well as the higher static stiffness for bearing working at gap between 5 and 12 μm; this is an ample film thickness designed for most aerostatic thrust bearings.

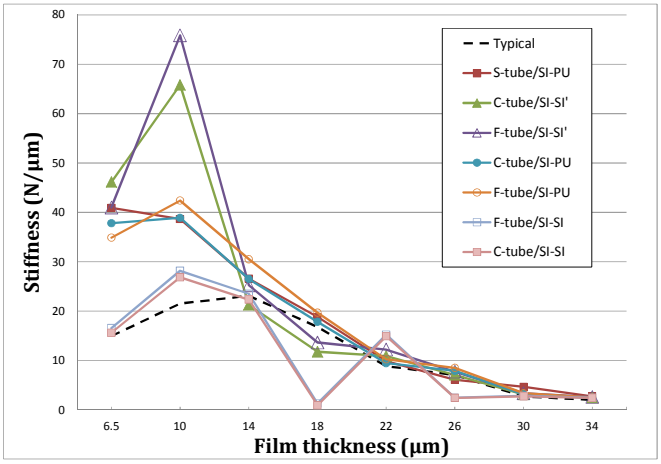

Fig. 4 Static stiffness vs. film thickness for various bearing structures and materials (S= straight; C= confined; F= free)

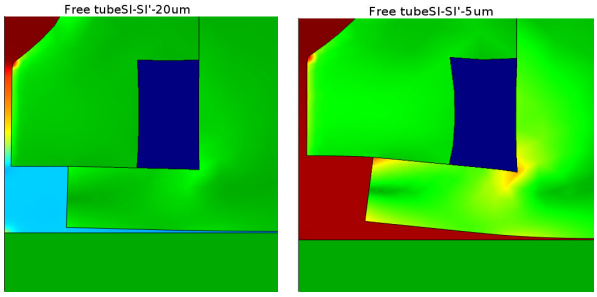

Fig. 5 Schematic presentation of the deformation and air pressure near the center part of free-tube/SI-SI' bearing. Film thicknesses equal to 20 (left) and 5 microns (right), respectively

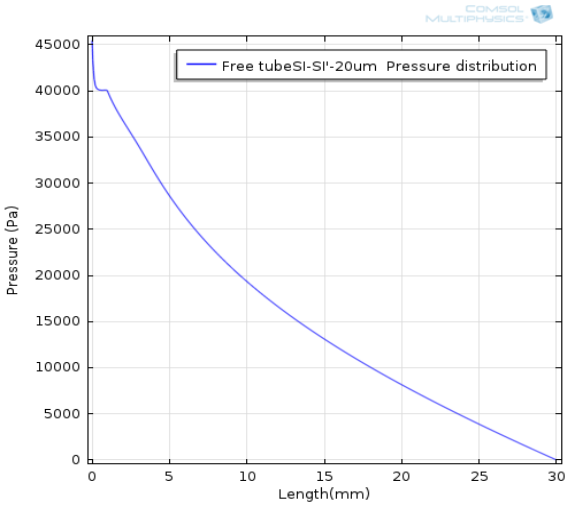

(a) Pressure distribution from disk center to outer rim

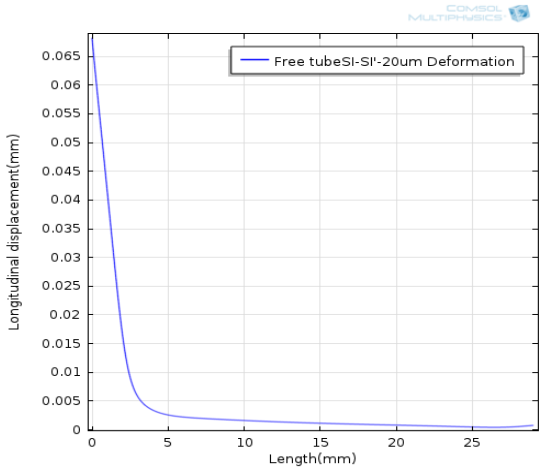

(b) Axial (longitudinal) displacement of bearing surface. Length is measured from air pocket edge to disk outer rim, total 29 mm

Fig. 6 Free-tube/SI-SI' bearing at film thicknesses 20 microns

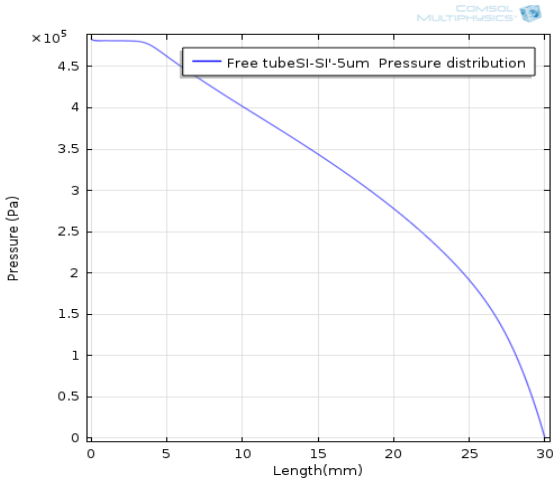

(a) Pressure distribution from disk center to outer rim

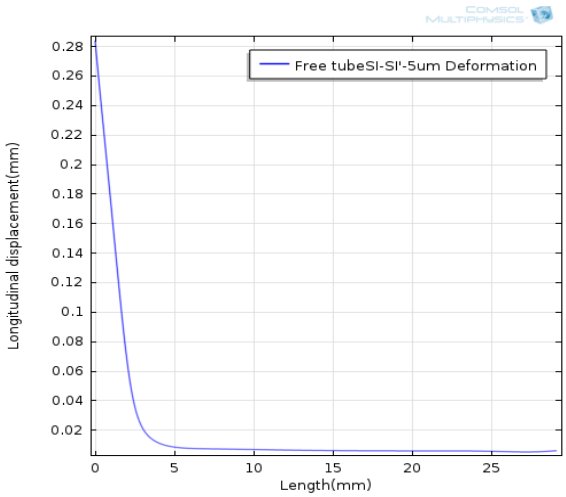

(b) Axial (longitudinal) displacement of bearing surface. Length is measured from air pocket edge to disk outer rim, total 29 mm

Fig. 7 Free-tube/SI-SI' bearing at film thicknesses 5 microns

ACKNOWLEDGMENT

The authors wish to thank the National Yunlin University of Science and Technology for the use of its facilities. The support from the National Science Council under grant NSC 102- 2221- E- 224- 014- MY3 is also gratefully acknowledged.

REFERENCES

[1] Y.-B. P. Kwan and J.B. Post, "A tolerancing procedure for inherently compensated, rectangular aerostatic thrust bearings," *Tribology International*, vol. 33, pp. 581-585, 2000.

[2] F. Al-Bender, "On the modelling of the dynamic characteristics of aerostatic bearing films: From stability analysis to active compensation," *Precision Engineering*, vol. 33, pp. 117-126, 2009.

[3] G. Aguirre, F. Al-Bender, and H. Van Brussel, "A multiphysics model for optimizing the design of active aerostatic thrust bearings," *Precision Engineering*, vol. 34, pp. 507-515, 2010.

[4] T. Aoyama, Y. Kakinuma, and Y. Kobayashi, "Numerical and experimental analysis for the small vibration of aerostatic guideways," *Annals of the CIRP- Manufacturing Tech.*, vol. 55 (1), pp. 419-422, 2006.

[5] S. Yoshimoto and K. Kohno, "Static and dynamic characteristics of aerostatic circular porous thrust bearings (effect of the shape of the air supply area)," *ASME Trans., J. Tribology*, vol. 123 (3), pp. 501-508, 2001.

[6] G. Belforte, T. Raparelli, V. Viktorov, and A. Trivella, "Metal woven wire cloth feeding system for gas bearings," *Tribology International*, vol. 42, pp. 600-608, 2009.

[7] Y. Li and H. Ding, "Influences of the geometrical parameters of aerostatic thrust bearing with pocketed orifice-type restrictor on its performance," *Tribology International*, vol. 40, pp. 1120-1126, 2007.